

Mixed convection casson fluids with the effects of porosity and radiation

N.F.M Omar¹, Z. Ismail^{1*}, R. Jusoh¹, R. A. Samah², H.I. Osman¹ and A.Q. Mohamad³,

¹Centre for Mathematical Sciences, Universiti Malaysia Pahang, Lebu Persiaran Tun Khalil Yaakob, 26300 Kuantan, Pahang, Malaysia

²Faculty of Chemical and Process Engineering Technology, Universiti Malaysia Pahang, Lebu Persiaran Tun Khalil Yaakob, 26300 Kuantan, Pahang, Malaysia

³Department of Mathematical Sciences, Faculty of Science, Universiti Teknologi Malaysia, 81310 Johor Bahru, Johor, Malaysia

ABSTRACT – The analysis of mixed convection Casson fluid with the effect of porosity and radiation was conducted. The governing partial differential equations (PDE) in dimensional form were formulated with associated initial and boundary conditions. The PDE were transformed into dimensionless form by presenting suitable non-dimensional variables. The temperature and velocity profiles were obtained by employing the method of Laplace transform, to ensure that initial and boundary conditions involved were satisfied. The graphical representation illustrates the effects of parameters for Casson fluid, porous medium and Grashof (Gr) number, in addition to radiation. It is inferred that at the start, the velocity decreases. However, at some point the velocity rises when the Casson parameter increases. Additionally, the increasing of radiation and Grashof number has influenced the velocity to increase.

ARTICLE HISTORY

Received: 20/07/2022

Revised: 21/09/2022

Accepted: 30/09/2022

KEYWORDS

Casson fluid

Laplace transform

Radiation

Porosity

Grashof number

INTRODUCTION

The Casson fluid model, proposed by Casson in 1959, was developed to elucidate the flow properties of pigment–oil suspensions [1]. The Casson fluid's shear stress and strain connection gives its non-Newtonian rheological features. With its elevated shear viscosity and yield stress, this fluid becomes an ideal indicator for applications that require shear thinning behaviour [2]. With the existence of thermal radiation, Pramanik [3] investigated the heat transfer and flow of Casson fluid over an exponentially porous stretched surface. Later, through an accelerating plate, Shahrim et al. [4] examined the exact Casson fluid solution for fractional convection and found that velocity would increase when Gr and time (t) increased. However, when Pr and β decreased, velocity decreased too.

Thermal radiation, a heat transfer phenomenon driven by electromagnetic waves, occurs due to significant temperature variations between two mediums. This process is pivotal in various technological endeavours involving exceedingly high temperatures. Fields such as space technology, power plants, furnace design, nuclear reactors, and glass production, among others, witness the influence of thermal radiation on fluid flow and thermal expansion dynamics [5]. The influence of thermal radiation has the potential to be used in numerous engineering and industrial applications, including astrophysical flows, nuclear energy plants, power generation, solar systems, gas production and space vehicles [6]. The radiative heat flux is applied by the Rosseland approximation in the energy equation [7]. Kumar et al. [8] investigated the impact of thermal radiation on magnetohydrodynamic (MHD) Casson fluid flow past an exponentially stretching curved sheet and observed that the presence of radiation led to an increase in temperature, and the thermal conductivity became temperature-dependent, along with irregular heat parameters. Additionally, the Casson parameter tends to inhibit momentum distribution, while the curvature parameter shows an opposite trend. Some of the interesting results can be found in [9 – 11].

The application of a porous medium efficiently regulates fluid velocity and facilitates heat transport in diverse industrial, agricultural, and manufacturing systems [12]. For instance, it plays a crucial role in applications like paper manufacturing, oil prospecting, and discarding radioactive waste materials. Conventionally, Darcy's law explains the properties of this medium; a modified Darcy–Forchheimer model is employed for addressing high-velocity flow issues. Porous medium flows are significantly relevant in oil recovery, trickle bed chromatography, cell technologies, drying techniques, material processing, and other fields [13]. Dash et al. [14] considered Casson fluid flow in a pipe filled with a homogeneous porous medium. Wahid et al. [15] acknowledged the influence of MHD Casson fluid flow and heat transmission in a porous medium across a stretching surface with slip condition and porosity parameter enhancing temperature profile.

Inspired from the above research, this study will cover the effects of porosity and radiation embedded in Casson fluids. Analytical solutions for all governing equations will be solved by using Laplace transform. Graphical results are presented using Mathcad and limiting cases have been done to ensure the results are parallel with previous findings.

METHODOLOGY

This research aims to achieve solutions in the occurrence of radiation and porous medium. The mixed convection Casson fluid adjacent to an accelerated plate positioned within a flow confined to the region at $x > 0$, where x is the magnitude of coordinate in the surface's normal direction. Initially, at $t = 0$, at a constant temperature, both the fluid and the plate are in a stationary state with accelerated plate velocity $u' = At$ at $t > 0$. The plate temperature is raised from T' to T'_w at the same time too.

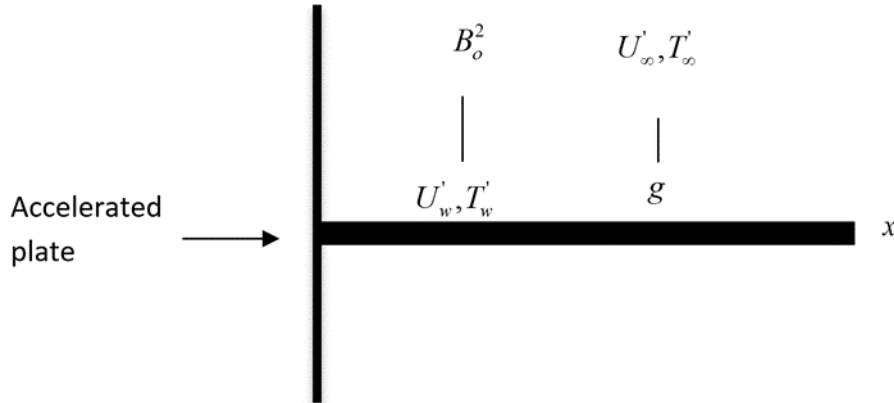


Figure 1. Physical configuration and system of coordinate

The governing dimensional momentum and energy equations are written as:

$$\rho \frac{\partial u'}{\partial t'} = \mu \left(1 + \frac{1}{\gamma} \right) \frac{\partial^2 u'}{\partial x'^2} + \rho g \beta (T' - T'_\infty) - \sigma B_o^2 u' - \frac{\nu}{K} u' \tag{1}$$

$$\rho c_p \frac{\partial T'}{\partial t'} = k \frac{\partial^2 T'}{\partial x'^2} - \frac{\partial q'_r}{\partial x'} \tag{2}$$

where γ represents the Casson fluid parameter, u' is denoted as fluid velocity in the x -direction, t is the time variable, ρ is the fluid density, μ is the dynamic viscosity, β is the coefficient of the thermal expansion, T' is the fluid temperature close to the plate, while T'_w is the temperature of the plate, B_o denotes the external magnetic field, ν represents the kinematic viscosity, k is the thermal conductivity, K is the porosity, c_p is the specific heat at constant pressure, and q'_r is the radiative heat flux. The associated initial and boundary conditions are as follows:

$$\begin{aligned} u'(x', 0) &= 0; & u'(0, t') &= At; & u'(\infty, t') &= 0; \\ T'(x', 0) &= T'_\infty; & T'(0, t') &= T'_w; & T'(\infty, t') &= T'_\infty, \end{aligned} \tag{3}$$

with dimensionless variable

$$u = \frac{u'}{(vA)^{\frac{1}{3}}}; \quad t = \frac{t' A^{\frac{2}{3}}}{v^{\frac{1}{3}}}; \quad x = \frac{x' A^{\frac{1}{3}}}{v^{\frac{2}{3}}}; \quad T = \frac{T' - T'_\infty}{T'_w - T'_\infty} \tag{4}$$

Rewrite back equations (1) and (2),

$$\rho A \frac{\partial u}{\partial t} = \mu \left(1 + \frac{1}{\gamma} \right) \frac{A}{\nu} \frac{\partial^2 u}{\partial u^2} + \rho g \beta (T'_w - T'_\infty) - \sigma B_o^2 u (vA)^{\frac{1}{3}} - \frac{\nu}{k} u (vA)^{\frac{1}{3}}, \tag{5}$$

$$\frac{\rho c_p \nu \partial T}{k \partial t} = \frac{\partial^2 T}{\partial x^2} + \frac{16 \sigma^* T'^3}{3k^* k} \frac{\partial^2 T}{\partial x^2}, \tag{6}$$

with the parameters applied in this research as follows:

$$Gr = \frac{g\beta(T_w - T_\infty)}{A}; \quad N = \frac{16\sigma^* T_\infty'^3}{3kk^*}; \quad Pr = \frac{\mu c_p}{k}. \tag{7}$$

Here, Gr indicates the thermal Grashof number, Pr for the Prandtl number, and N is the radiation. Therefore,

$$\frac{\partial u}{\partial t} = \left(1 + \frac{1}{\gamma}\right) \frac{\partial^2 u}{\partial x^2} + GrT - \sigma B_o^2 \frac{uv^{\frac{1}{3}}}{\rho A^{\frac{2}{3}}} - \frac{v}{k} \frac{uv^{\frac{1}{3}}}{\rho A^{\frac{2}{3}}}, \tag{8}$$

$$\frac{\partial T}{\partial t} = \frac{(1+N)}{Pr} \frac{\partial^2 T}{\partial x^2}. \tag{9}$$

By using Laplace transform for equations (8) and (9),

$$\left(1 + \frac{1}{\gamma}\right) \frac{d^2 \bar{u}}{dx^2} - \left(s + \frac{\sigma B_o^2 v^{\frac{1}{3}}}{\rho A^{\frac{2}{3}}} + \frac{v}{k} \frac{v^{\frac{1}{3}}}{\rho A^{\frac{2}{3}}}\right) \bar{u} = -Gr\bar{T}, \tag{10}$$

$$\frac{d^2 T}{dx^2} - aT = 0, \quad a = \frac{Pr}{1+N}. \tag{11}$$

Equations (10) and (11) are derived by applying the inverse Laplace transform as follows:

$$\begin{aligned} u(x,t) = & \frac{1}{2} e^{x\sqrt{zL}} \operatorname{erfc}\left(\frac{x}{2}\sqrt{\frac{z}{t}} + \sqrt{Lt}\right) + e^{-x\sqrt{Lz}} \operatorname{erfc}\left(\frac{x}{2}\sqrt{\frac{z}{t}} - \sqrt{Lt}\right) + \\ & \left[-\frac{1}{2j} e^{x\sqrt{zL}} \operatorname{erfc}\left(\frac{x}{2}\sqrt{\frac{z}{t}} - \sqrt{Lt}\right) + e^{-x\sqrt{Lz}} \operatorname{erfc}\left(\frac{x}{2}\sqrt{\frac{z}{t}} + \sqrt{Lt}\right)\right] + \\ & \frac{1}{j} \operatorname{erfc}\left(\frac{x}{2}\sqrt{\frac{9}{t}}\right) + \left[\frac{e^{jt}}{2j} e^{x\sqrt{z(L+j)}} \operatorname{erfc}\left(\frac{x}{2}\sqrt{\frac{z}{t}} + \sqrt{t(L+j)}\right) + \right. \\ & \left. e^{-x\sqrt{z(L+j)}} \operatorname{erfc}\left(\frac{x}{2}\sqrt{\frac{z}{t}} - \sqrt{t(L+j)}\right)\right] + \left[-\frac{1}{j} \frac{e^{jt}}{2} e^{x\sqrt{aj}} \operatorname{erfc}\left(\frac{x}{2}\sqrt{\frac{a}{t}} + \sqrt{jt}\right) + \right. \\ & \left. e^{-x\sqrt{aj}} \operatorname{erfc}\left(\frac{x}{2}\sqrt{\frac{a}{t}} - \sqrt{jt}\right)\right] \end{aligned} \tag{12}$$

$$T(x,t) = \operatorname{erfc}\left(\frac{x\sqrt{a}}{2\sqrt{t}}\right) \tag{13}$$

RESULTS AND DISCUSSION

Prior to delving into the parameters considered in this study, it is significant to ensure that the solutions have a precise and accurate understanding of the model employed, particularly in comparison to past studies. Before further discussion, it is vital to validate this research with past studies to ensure it is correctly executed. From Figure 2, comparison from Shahrin et al. [4] has been done for the velocity field with respect to time, t . The validation shows good agreement with the studied problem. For that, we are sure the solutions obtained are accurate.

The graphs presented in this study were plotted using different values of embedded parameters to analyse their impacts on velocity and temperature profiles. Figure 3 specifically focuses on time. Figures 4 to 7 assess the velocity profiles and the effects of Casson fluid parameter, radiation, porosity, and Grashof number.

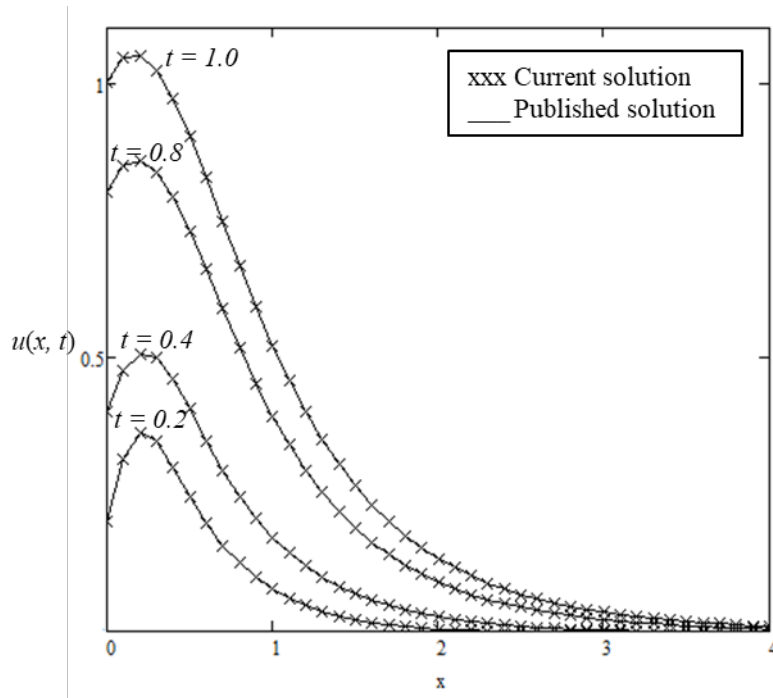


Figure 2. Validation results from published solution, Shahrin et al. [4]

The influence of time on the temperature profile is presented in Figure 3, revealing a significant increase in temperature. The graph generally displays a distinct pattern where temperature surges with the progression of time. This pattern can be ascribed to the escalating energy produced by the fluid flow, as indicated by the observed trend in the graph.

Figure 4 depicts the effect of the Casson fluid parameter on the velocity profile. Initially, the velocity experiences a rise, but at a certain point, it starts to decline gradually. This behaviour is a distinctive characteristic of Casson fluids. As the Casson fluid parameter rises, and over time too, the fluid’s shear stress gradually exceeds the yield stress, resulting in an upsurge in the thickness of the boundary layer.

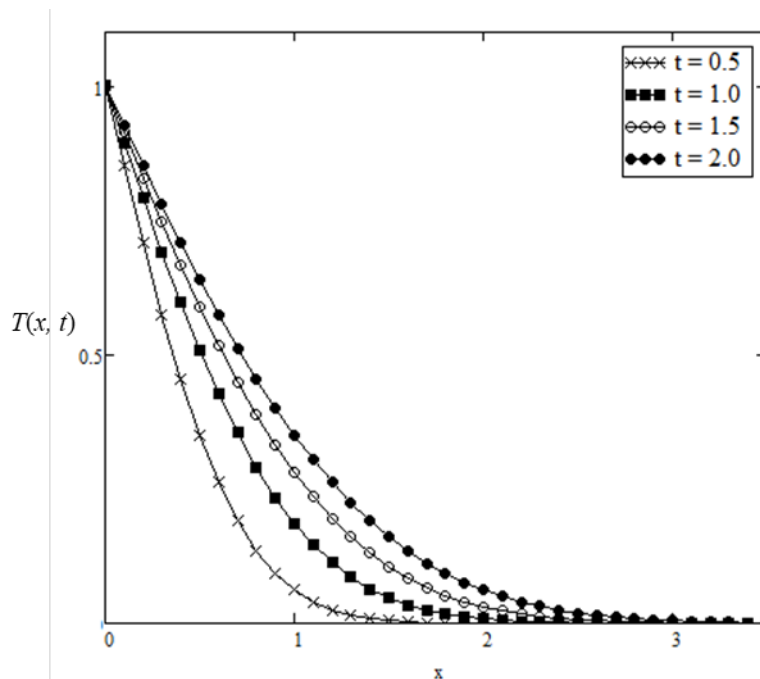


Figure 3. Temperature profiles with different t

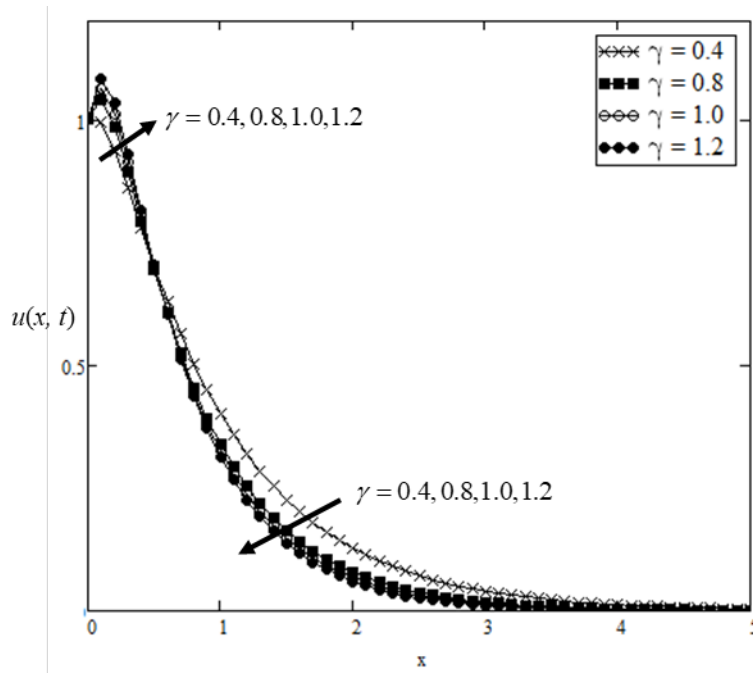


Figure 4. Velocity profiles with different γ

Figure 5 delineates the fluid velocity profiles for varying values of thermal radiation N . It is ascertained that the velocity increases with increasing values of N in the existence of thermal radiation. This observation is expected because higher radiation occurs when the temperature increases, and as an impact, the velocity increases. The results demonstrate that higher radiation intensity leads to an increase in velocity. The fluid's temperature rises when the radiation intensity is high because more heat is delivered to it. A higher kinetic energy results in a higher velocity when the fluid's temperature rises. An increase in K is associated with reduced velocity (Figure 6). This outcome can be elucidated by considering Darcy's law, which asserts that the existence of a porous medium reduces the flow resistance and consequently promotes fluid motion. Thus, the graph confirms the significant role of porosity in the current analysis.

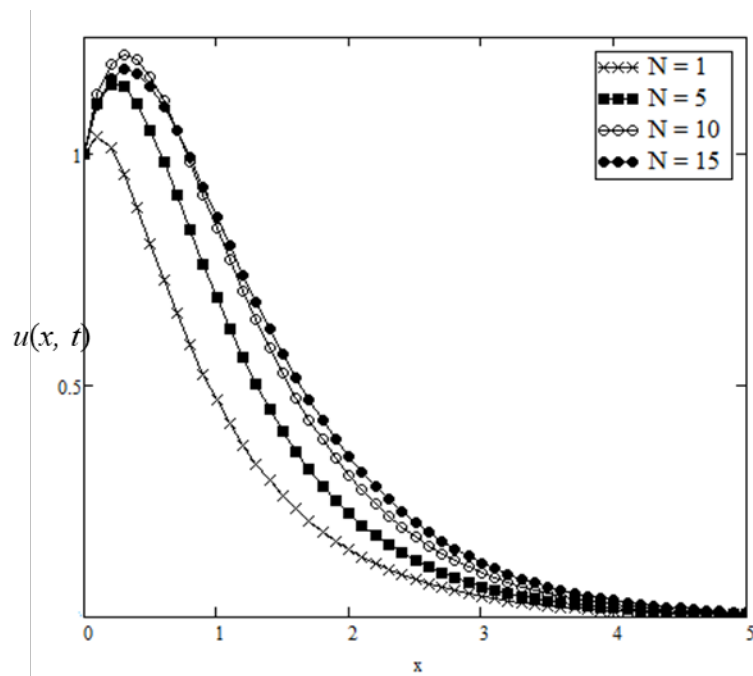


Figure 5. Velocity profiles with different N

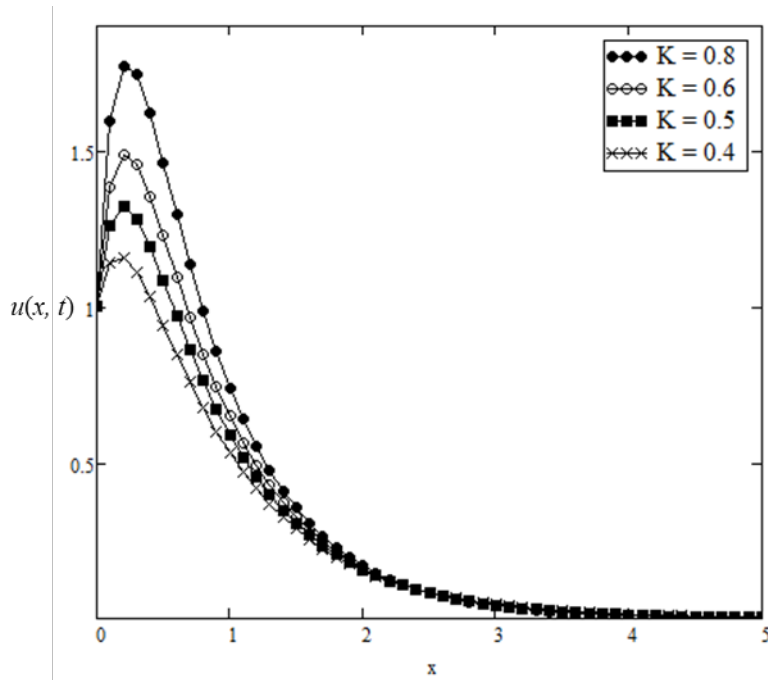


Figure 6. Velocity profiles with different K

Figure 7 illustrates the impact of the Grashof number (Gr) on the velocity profile, representing the proportionate influence of thermal buoyancy force over the viscous hydrodynamic force. A gradual increase in velocity is observed as the Grashof number rises. This phenomenon occurs due to the heightened buoyancy force in the flow, leading to an overall augmentation in fluid velocity.

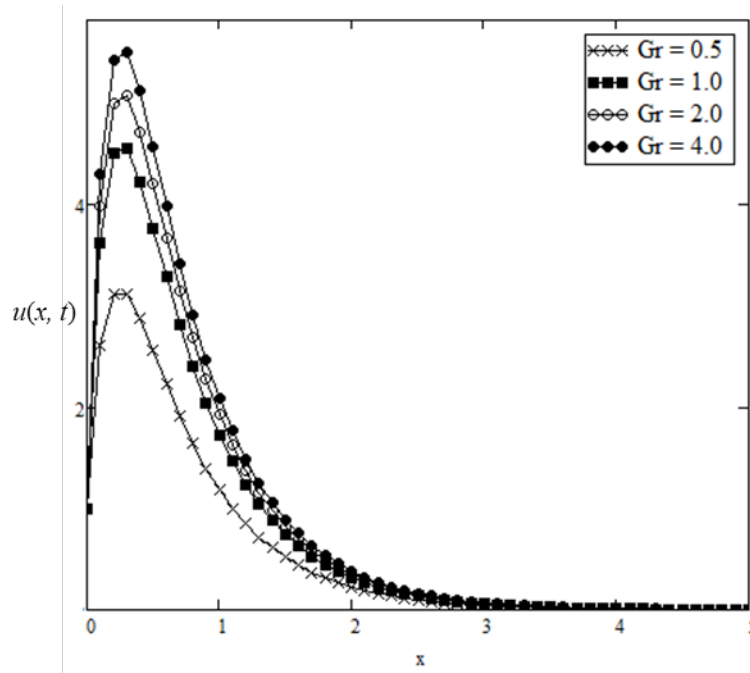


Figure 7. Velocity profiles with different Gr numbers

CONCLUSION

This study enlightens the implications of porosity and radiation to the mixed convection Casson fluid model. The analysis was done mathematically with the execution of the Laplace transform. Temperature profiles are escalated with time (t), whereas the velocity profiles exhibit various patterns with the increment in the Casson fluid parameter. The velocity initially lifts, but it progressively decreases after a while. Additionally, it is observed that the velocity profiles exhibit an increase in response to radiation and Grashof number, while they decrease due to the porosity effect.

ACKNOWLEDGEMENT

The authors would like to acknowledge Universiti Malaysia Pahang (UMP) for the financial support via vote number UIC221516 for this research.

REFERENCES

- [1] N. Casson, "A flow equation for the pigment oil suspensions of the printing ink type," *Rheology of Disperse Systems*, pp. 84–102, 1959.
- [2] M. Shoaib, M. Kausar, K.S., Nisar, M.A.Z., Raja, A. Morsy, "Impact of thermal energy on MHD Casson fluid through a Forchheimer porous medium with inclined non-linear surface: A soft computing approach," *Alexandria Engineering Journal*, vol.61, pp. 12211-12228, 2022.
- [3] S. Pramanik, "Casson fluid flow and heat transfer past an exponentially porous stretching surface in presence of thermal radiation," *Ain Shams Engineering Journal*, vol.5, pp. 205-212, 2013.
- [4] M.N. Shahrim, A.Q. Mohamad, L.Y. Jiann, M.N. Zakaria, S. Shafie, Z. Ismail, A. R.M. Kasim, "Exact Solution of Fractional Convective Casson Fluid Through an Accelerated Plate," *CFD Letters.*, vol.13, no. 6, pp. 15-25, 2021.
- [5] M.M., Alqarni, M. Bilal, R. Allogmany, E. Tag-Eldin, M.E. Ghoneim, M.F. Yassen, "Mathematical analysis of Casson fluid flow with energy and mass transfer under the influence of activation energy from a non-coaxially spinning disc," *Frontiers in Energy Research.*, pp. 10: 986284, 2022.
- [6] A. Sahoo, R. Nandkeolyar, "Entropy generation and dissipative heat transfer analysis of mixed convective hydromagnetic flow of a Casson nanofluid with thermal radiation and Hall current," *Scientific Reports.*, pp. 11:3926, 2021.
- [7] S.G., Bejawada, Y.D., Reddy, W, Jamsheed, K.S., Nisar, A.N., Alharbi, R. Chouikh, "Radiation effect on MHD Casson fluid flow over an inclined non-linear surface with chemical reaction in a Forchheimer porous medium," *Alexandria Engineering Journal.*, vol. 61, pp. 8207-8220, 2022.
- [8] K. Anantha Kumar, V, Sugunamma, N. Sandeep, N., "Effect of thermal radiation on MHD Casson fluid flow over an exponentially stretching curved sheet," *Journal of Thermal Analysis and Calorimetry*, pp. 140: 2377–2385, 2019.
- [9] A. Hussanan, S. Aman, Z. Ismail, M.Z. Salleh B., Widodo. "Unsteady natural convection of sodium alginate viscoplastic casson based based nanofluid flow over a vertical plate with leading edge accretion/ablation". *Journal of Advanced Research in Fluid Mechanics and Thermal Sciences.* vol. 45, no.1, pp. 92-8, 2018.
- [10] M. Sohail, Z. Shah, A. Tassaddiq, P. Kumam, P. Roy, "Entropy generation in MHD Casson fluid flow with variable heat conductance and thermal conductivity over non-linear bi-directional stretching surface". *Scientific Reports.* vol. 27, no.10(1), pp. 12530, 2020.
- [11] T. Anwar, K, Poom, W. Wiboonsak, "Unsteady MHD natural convection flow of Casson fluid incorporating thermal radiative flux and heat injection/suction mechanism under variable wall conditions." *Scientific Reports*, vol.11,no.1, pp. 4275, 2021.
- [12] A.M. Siddiqui, Q.A. Azim, "Creeping flow of a viscous fluid in a uniformly porous slit with porous medium: an application to the diseased renal tubules," *China Journal of Physics*, vol. 64, pp. 264–277, 2020.
- [13] J.C. Zhou, A. Abidi, QH Shi, M. R. Khan, A. Rehman, A. Issakhov, A. M. Galal, "Unsteady radiative slip flow of MHD Casson fluid over a permeable stretched surface subject to a non-uniform heat source," *Case Studies in Thermal Engineering.*, vol. 26, pp. 101141, 2021.
- [14] K. Dash, G. Mehta, G. Jayaraman, "Casson fluid flow in a pipe filled with a homogeneous porous medium," *Int. J. Eng. Sci.*, vol. 34, pp. 1145-1156, 1996.
- [15] N.S. Wahid, N.M. Arifin, M. Turkyilmazoglu, N.A.A Rahmin and M.E.H Hafidzuddin, "Effect of magnetohydrodynamic Casson fluid flow and heat transfer past a stretching surface in porous medium with slip condition," *Journal of Physics: Conference Series*, pp. 012028, 2019.